The Canadian Society for Bioengineering
The Canadian society for engineering in agricultural, food, environmental, and biological systems.

CSBE | SCGAB

La Société Canadienne de Génie Agroalimentaire et de Bioingénierie
La société canadienne de génie agroalimentaire, de la bioingénierie et de l'environnement

Paper No. CSBE17125

The effect of compaction on pore structure in bulk grains

C. Nwaizu
Graduate Student, Department of Biosystems Engineering, University of Manitoba, Winnipeg, MB, R3T 5V6, Canada.

Q. Zhang
Professor, Department of Biosystems Engineering, University of Manitoba, Winnipeg, MB, R3T 5V6, Canada.

Written for presentation at the
CSBE/SCGAB 2017 Annual Conference
Canada Inns Polo Park, Winnipeg, MB
6-10 August 2017

ABSTRACT Experiments were conducted to determine the effect of compaction due to grain depth on porosity, tortuosity and connectivity of pore structure within bulk grains. Wax was used to "freeze" the pore structure to allow the grain samples to be cut and the internal structures to be imaged. The acquired images were analyzed by using a 3-D image reconstruction technique to determine various pore structure parameters. Results indicated that porosity decreased with the grain depth (compaction pressure), with the initial porosity being 0.41 and decreased to 0.34 at a pressure equivalent to a 5 m grain depth. Tortuosity increased with grain depth from 1.17 initially to 1.57 at a 5 m grain depth, or 34%. Models were developed based on 3-D experimental data to predict variations in porosity and tortuosity as a function of grain depth. Model predictions were within 5% of experiment data.

Keywords: Bulk grains, Pore structure, Porosity, Tortuosity, Compaction

INTRODUCTION

The pore structure is a fundamental property of porous materials, such as bulk grains, and it dictates the resistance to airflow. A common assumption is that the pore structure is uniform in a grain bed when designing grain dry and aeriation systems. However, as a porous material, bulk grains may have variable pore structure, as affected by pressure to which it subjected (or by the grain depth). Haque (2011) showed that considering the effect of decrease in void fraction with grain depth would result in higher airflow resistance than that reported by Shedd (1953) for cereal grains. Therefore, assuming a simple, constant, and homogeneous pore structure for bulk grains can lead to inaccurate estimation/prediction of physical parameters involved in aeration or drying processes, such as airflow velocity and static pressure distribution (Khatchatourian and Savicki, 2004). Yue and Zhang (2017) stated in their study that assuming a constant grain bed viodage (pores) would create serious errors in predicting airflow characteristics in bulk grains. Realistic mathematical modeling of flow through bulk grains can only be achieved when transport equations are developed to account for the structural and geometrical complexities of the pore structure. Hihinashvili and Blumenfeld (2010) concluded that establishing this pore structure-transport relationship, which they referred to as one of the "holy grails" in this field of study, is the key in accurately predicting flow and macroscopic properties.

The inherent heterogeneity and the spatial changing in the arrangement of pores create extreme complexity in quantifying pore structure inside bulk grains (Neethirajan et al. 2008). Therefore, to understand airflow distribution through bulk grains, the first step is to characterize the intricate nature of pore network, and secondly, to be able to map spatial changes in pore structure characteristics along the grain beds.

Recently, few studies have tried to integrate variability in pore structure for predicting airflow and pressure drop in bulk grains. Garg (2005) used Ergun's equation for modeling non-uniform airflow where variable porosity was represented with two different values, one for the center core volume of the grain mass and the other for the peripheral volume. Lawrence and Maier (2012) and Olatunde et al. (2016) used two different porosity values, one at the center and the other at the wall, and assumed that porosity varied linearly from the center to the wall in their studies of three-dimensional airflow distribution in stored maize and rice grains. Neethirajan et al. (2006) had successfully used X-ray CT to scan and image small grain samples to reconstruct the 3-D internal pore structures of wheat, peas and barley. CT imaging techniques also have their limitations. High spatial resolution limits the sampling area and does not produce a good representative of large-scale changes in heterogeneity of the pore structure. Conversely, low spatial resolution X-ray CT imaging increases the sampling area but over-estimates the pore sizes (Peng et al. 2012).

The objective of this research were to: (1) develop a method for quantifying the pore structure of bulk grains; (2) determine the effect of compaction on the pore structure of a bulk grain; and (3) develop pore structure models using a 3-D Image reconstruction technique for predicting porosity and tortuosity due to compaction in grain beds

MATERIALS AND METHODOLOGY

Experimental setup and procedures

The experiment was conducted by using a rigid cylindrical model bin of 0.28 m height and 0.15 m diameter, made with sheet steel. The grain used in this study was soybeans. The grain moisture content was determined by using the standard oven method as outlined in the ASABE Standard: 105°C for 72 hours (ASAE R2008.S352.2, 2004). The moisture content was obtained as 8.82% (WB).

In each test, soybean was filled into the model bin to a depth of 0.12 m through a funnel placed 0.1 m above the bin (fig. 1). This filling procedure was used to ensure a reproducible structure of the soybean grain bed. A similar filling procedure was used by Molenda et al. (2005) to ensure that bulk density of grain bed did not change in all their experimental runs. After filling, the grain developed a heap, which was gently leveled manually. Dead weights were applied on the top surface to apply the over-burden pressure to compact the grain to simulate the grain depth effect, Janssen's (1895) equation was solved to determine the vertical pressures in a 10-m diameter bin, based on which the amounts of dead weights were determined. The simulated grain depths were 2, 5, 10, 15, 20, and 25 m.

After a dead load was applied, the grain continued to settle until a stable state was reached. A preliminary test was carried out to determine the duration at which no further compaction would occur under the given load. The result showed that the grain bed stabilized after 48 hours. In the subsequent tests, all the measurements were taken 48 hrs after the dead load was applied.
Colored paraffin wax was used to "freeze" the pore structure before the sample was cut and imaged for analysis. Specifically, once the grain bed was stabilized, a wax bar was melted to form liquid wax, which was then gently poured into the grain bed (bin). The wax was then allowed to harden at room temperature. The solidified grain bed was then taken out from the model bin by releasing the metal buckles of the bin. An electrical cutting saw was used to cut three cylindrical sub-samples ((0.15 m diameter and 0.04 m height) from the top, middle and bottom region of the solidified grain bed. Each compaction condition was replicated three times.

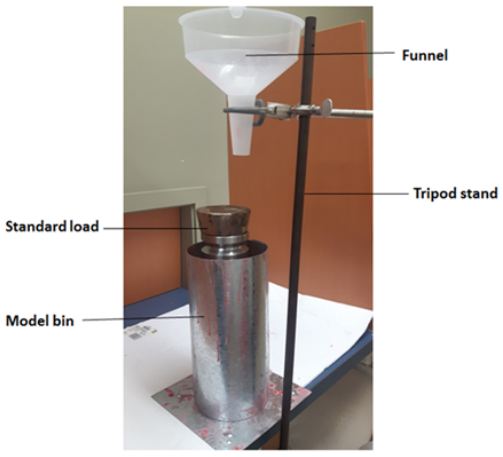

Figure1: Experimental set-up for the compaction test

Image acquisition, segmentation and quantifications

Immediately after cutting the sub-samples from the solidified grain bed, surfaces of the of the sub-samples were cleaned gently with soft paper and an image of the cross section was acquired with an HD camera (Exilim EX-F1 Casio Computers Co., Ltd, Tokyo, Japan). These images were late processed and used for quantifying the 2-D parameters of the pore structures. For the 3-D reconstruction, each of the sub-samples was further cut into discs of 0.02m thickness and the surfaces of discs were imaged.

The acquired images were processed with Image J, image processing software developed by the United State National Institute of Health (NIH, Bethesda, MD, US). The image analysis procedures used in this study were grouped into four main steps: Pre-processing, Segmentation, 3-D volume reconstruction, and pore detection and measurement.

All images were resized to 625 × 521 pixel images to include the area with vivid details of the pores across the section (fig. 2). These RGB images were then converted into 8-bit images to ease the identification and quantification of pores during processing (fig. 2). A uniform contrast enhancement filter was applied to normalize all the section images and reduce the effect of differences in the pixels between neighboring sections.

Segmentation of an image is the process of separating each pixel of the image as being a member of any one of two or more set (Robertson et al. 1997). In this study, all the images of the sections were segmented based on a threshold value that separate the pixels that belong to the red colored (wax filled pores) from the grain kernels, and this created binary images with intensity value of 1 (white) for the particles (grain kernel) and 0 (black) for the pores in the image.

Several built-in thresholding algorithms in ImageJ such as Otsu's algorithm and Maximum Entropy algorithm were tested on the images. However, results obtained were not satisfactory based on visual inspections. So in this study, the method for selecting threshold value was subjective. The method involved increasing the gray-level value gradually until the binary image agrees with the visual inspection of the unedited image. Because of the marginal distribution of the pixel values representing grain kernels and the pixels representing the pores overlapped in the original 8-bit image, thresholding introduced a certain amount of noise into the binary image. This noise was mostly evident in pore-grain kernel boundaries, and manifested as a tiny pores or tiny kernel points within the pores. To reduce the presence of the noise, a morphological filter was applied to all the thresholded images. The filter operation consisted of two sequential applications, which were the erosion and dilation operations using the same morphological structural element to detect, modify or remove certain shape features in an image under consideration. For this operation, the same size of structural element that corresponded to the size of the noise features was used for the entire image.

Three dimensional (3-D) images were obtained by using the 3D beat plug-in, an ImageJ plug-In that could be used for reconstructing a 3-D volume from the 2-D image section stack after being aligned by StackReg, another ImageJ plug-in.

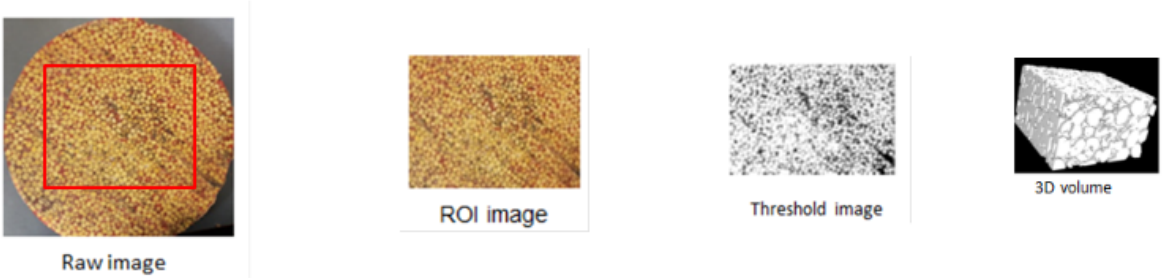

Figure 2: Steps in obtaining the 3-D volume image

Once the 3-D representations were obtained, critical pore structure parameters, such as porosity and tortuosity, related to flow through bulk grains were then quantified by the use of the 3-D beat plug-in. Another morphological filtering operation was applied to the 3-D image volume to fill holes and removed noise related artifacts that might appear after 3-D reconstruction of the images before quantitative evaluations of the pore structure parameters. The 3-D reconstruction not only provided a quantitative data sets for estimating tortuosity and porosity which were used in pore structure characterization; but also provided a means of visualization for the different pores and pore channels that exist inside the bulk grain.

The 3-D volume images were further processed by partitioning the pore space into pores based on the pore definition given by Dullien et al. (1989): a pore is a portion of the pore space bounded by a solid surface and planes erected where the hydraulic radius of the pore space exhibits local minima. The partition was carried out in such a way that all adjoining pores with no obvious geometrical connecting throat were identified and the boundary between the connected pores were separated using the watershed macro in ImageJ that implements an iterative algorithm based on a morphological thinning technique.

Once the pores have been accurately and unambiguously partitioned, their volume was then estimated based on the number of voxels in each individual partitioned pore.

For each of the 3-D volume obtained, porosity and tortuosity (based on connectivity parameter) were quantified.

Porosity was estimated as the ratio of the number of pore voxel to the total number of the voxels in the 3-D volume as stated below:

$$\varepsilon = \frac{V_{pv}}{V_{sv}} \tag{1}$$

where ε =porosity, V_p = total pore voxel, V_s = total sample voxel.

Connectivity between pores is one of the most important parameters of pore structure that relate to flow through porous materials. Researchers have used different methods in defining pore connectivity in porous media, such as coordination number, degree of connected pores, Euler value, Fragmentation index and so on (Vogel et al., 1997; Neethirajan et al., 2006; Nwaizu and Zhang, 2015). In this study, a different approach was proposed and used. Specifically, the image techniques were used to identify and extract the largest connected path from the reconstructed 3-D image volume of the bulk grain (fig. 3). The degree of connectivity was estimated based on the

volume ratio of the voxel of the largest connected path to the total sample voxels. This means that degree of connectivity within a given bulk grain was approximately equal to one if all the pores were connected and equal to zero when all the pores were not connected or isolated.

$$c = \frac{V_{lp}}{V_s} \tag{2}$$

where c =degree of connectivity, V_{lp} = voxel of the largest connected path, V_s = total sample voxel.

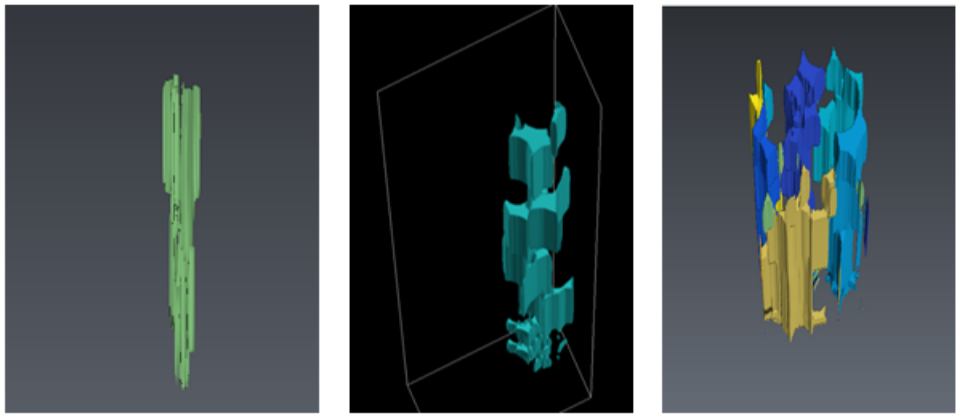

Figure 3: Example of a reconstructed volume of branch paths (a) and (b) and the largest connected path (c)

Tortuosity was then determined from the largest connected paths, as the ratio of average tortuous path lengths extracted from the largest connected path to the effective path length.

$$\hat{\tau} = \frac{\bar{L}_{lp}}{L_{eff}} \tag{3}$$

where τ =degree of connectivity, $\bar{L}_{lp}$ = voxel of the largest connected path, L_{eff} = total sample voxel. Before quantifying the tortuosity the 3-D reconstructed largest path volume were skeletonized with an ImageJ macro in order to obtain the effective path length as well as the flow path lengths of the individual possible paths (or branches) that made up the largest connected path. In this study, the average tortuosity estimated was termed geometrical branch tortuosity.

Statistical analysis

Statistical analyses were carried out with the SAS statistical software (Statistical Analysis Systems, Carry, NC) to analyze the experimental data. Analysis of variance (ANOVA) was applied to determine which of the factors had a significant effect on porosity and tortuosity. The factor was considered significant if $P < 0.05$ and Tukey test was employed to determine the significant between the means of the factors that had a significant effect on porosity and tortuosity. When experimental data were fit into mathematical models, fitting was done using the non-linear

regression functions with coefficient of determination (R^2) and the standard error of estimate (SEE) being used in evaluating the goodness of fit.

RESULTS AND DISCUSSION

Porosity

Porosity decreased with increase in the grain depth (compaction pressure) as expected (fig. 4). The rate of decrease in porosity was higher at the lower pressure and then gradually approached a minimum value. Without compaction pressure, the initial porosity was determined to be 0.41 and porosity reduced to 0.34 at a pressure equivalent to 0.5 m grain depth. This initial fast decrease in the porosity was probably because of the re-arrangement of the grain particles (Thompson and Ross, 1983).

Several models have been developed to model the variations in bulk density as functions of compaction pressure (Thompson et al. 1987; Hague, 2013; Cheng et al. 2015). Thompson et al. (1987) developed a computer program based on their model to estimate the packing densities of various grains, including sorghum, corn, rice, soybean, and wheat. Cheng et al. (2015) developed two models for predicting bulk density and bulk modulus as functions of equivalent compressive pressure and moisture content.

Based on the experimental data, an exponential function was proposed to model the variation of porosity was a function of grain depth:

$$\varepsilon_z = \varepsilon_o - B(1 - e^{-\propto z}) \tag{4}$$

where ε_z is the predicted porosity at a given depth, ε_o is the maximum porosity obtained at the surface of the grain bed ($z = 0$); B and $\propto$ are the empirical model parameters.

Using the SAS statistical NLIN procedure, parameter B was estimated to be 0.35 and $\propto$ 0.07. The model prediction compared well with the experimental data (fig. 4), with a relative error less than 5%.

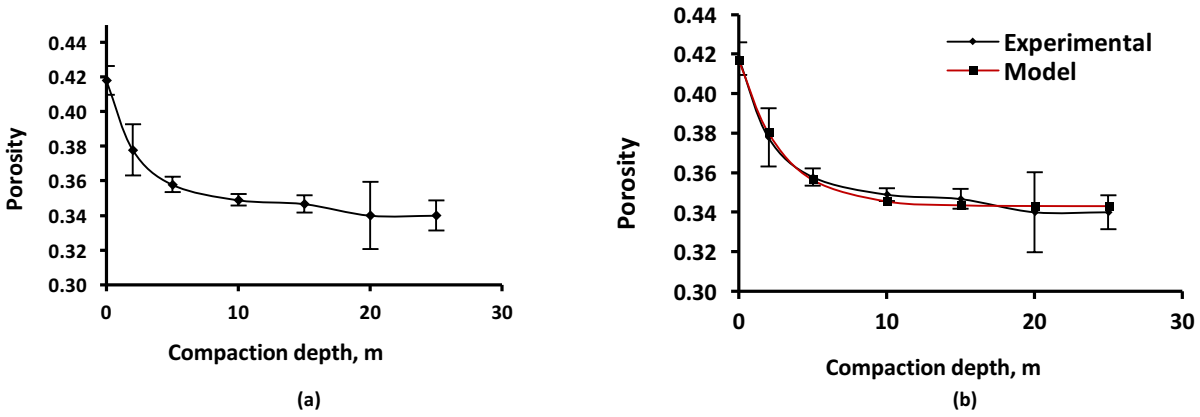

Figure 4: Comparison between the predicted model and experimental results

To further validate the model, the model prediction was compared with a data set reported in the literature by Khatchatourian et al. (2004) for soybeans stored in a lab-scale polyvinyl chloride bin with a diameter of 0.2 m and height of 1.0 m. The bin was contained in a wooden structural support equipped with lever-operated compacting device to apply force that could simulate up to 50 m depth of grain. Table 1 shows that predictions by the present model were in close agreement with the experimental data. The results were also compared with the prediction from an exponential mathematical model developed to determine void fractions at different depths of granular materials in deep beds by Haque et al. (2011).

Table 1: Prediction of porosity at various depths

Grain bed depth, m	Experimental Khatchatourian et al. (2004)	Model (Present study)	Model (By Haque et al)
1	0.391	0.397	0.353
5	0.385	0.359	0.343
10	0.382	0.349	0.332
20	0.375	0.347	0.319
30	0.371	0.347	0.311

Compaction would change not only porosity, but also pore size and shape. Pore sizes and shapes were examined at a grain depth of 25 m (high compaction), and 0 m (no compaction). The pore size was represented by the pore volume. The pore shape was evaluated by the sphereicity. Results indicated that compaction reduced pore sizes, resulted in more small pores (in 1 - 2 mm^3 range) and less large pored (> 3 mm^3) (fig. 5). Similar results were obtained from the experiment conducted by Robertson and Campbell (1997). Compaction created narrow constrictions in the pore space, which consequently would lead to the increase in number of the pores.

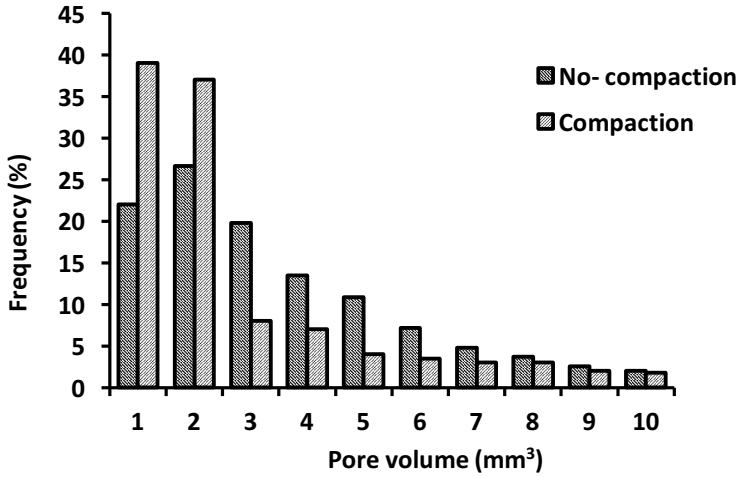

Figure 5: Comparison effect of no-compaction and compaction on pore volume.

Figure (6) shows the shape distribution for the pore structure estimated by the sphericity. The results indicated that compaction resulted in higher sphericity, meaning that more pores were close to being spherical in shape.

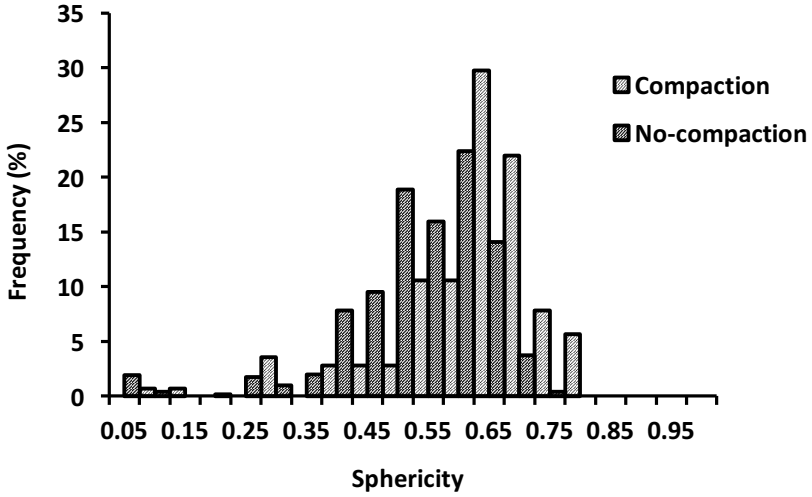

Figure 6: Effect of compaction and no-compaction on pore shape

Tortuosity and connectivity

Since flow would naturally follow the least resistance paths among the notoriously complex, bundles of flow paths that existed within the grain bed, the largest connective path was identified within the 3-D volume and its 3-D volume was reconstructed. Tortuosity was then estimated based on the largest connected paths. The estimated tortuosity increased with grain depth from 1.17 at 0 depths to 1.57 at 25 m, or 34% (fig. 7a).

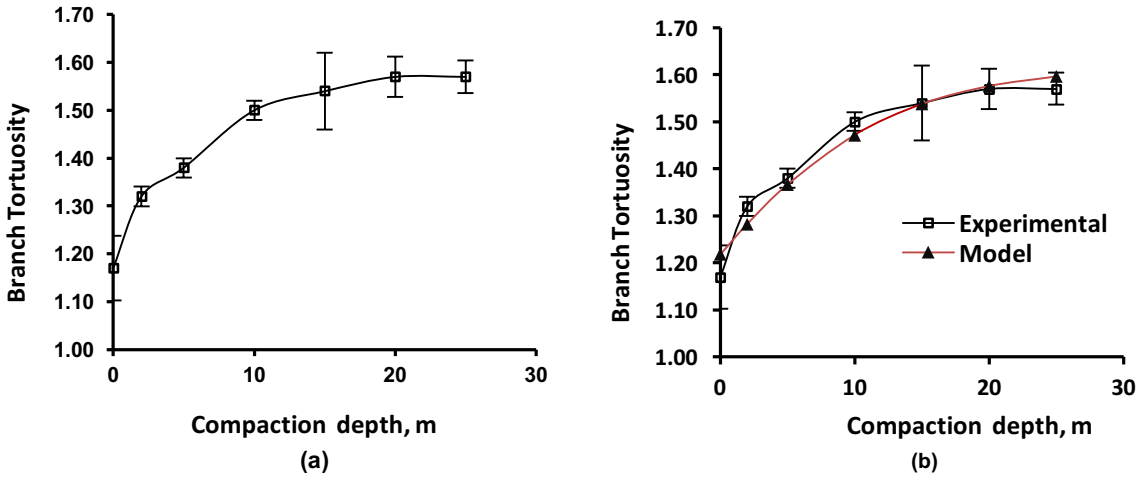

Figure 7: Variation in tortuosity with compaction depth

Many models have been proposed to correlate tortuosity to porosity. Based on a model proposed by Yun et al. (2005), we correlated the tortuosity to the grain depth as follows:

$$\tau = a - bln(\varepsilon_z) \tag{5}$$

where τ is the tortuosity, a and b empirical model parameters

Substituting equation (4) into (5) yields:

$$\tau_z = a - b\ln[\varepsilon_o - B(1 - e^{-\propto z})] \tag{6}$$

Using the SAS statistical NLIN procedure, the parameter a was estimated to be 0.95 and b 0.36. Model predictions compared well with the experimental data, with an overall relative error less than 5 % (fig. 7b).

While tortuosity describes the complexity involve along individual flow paths, the degree of connectivity helps to describe connections that exist between one or more branch flow paths. The results showed a general trend of decrease in the degree of connectivity with increasing tortuosity (fig. 8). In other words, as the grain depth increased, tortuosity increased and the degree of connectivity decreased.

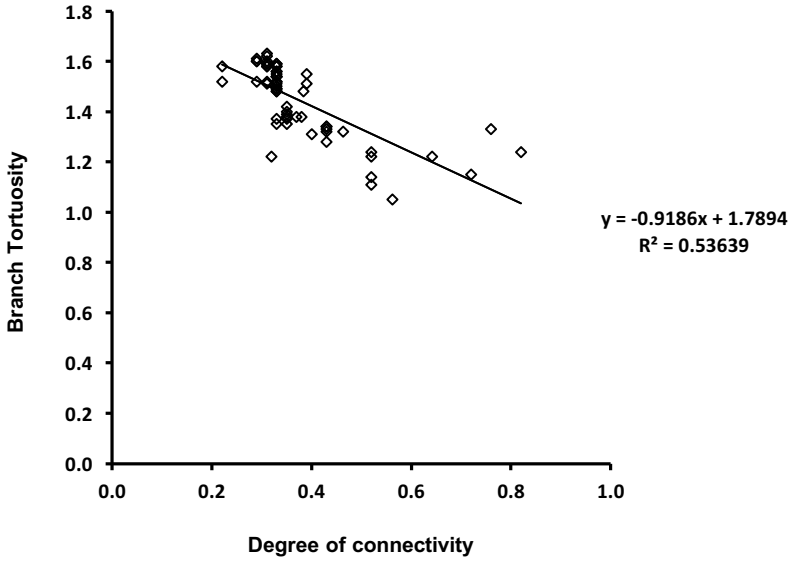

Figure 8: Relationship between tortuosity and degree of connectivity

CONCLUSION

.

1. The proposed method of the 3-D image reconstruction has potential of quantifying critical pore structure parameters such as porosity, tortuosity and pore connectivity in porous materials such as bulk grains.
2. The influence of compaction on porosity and tortuosity were clearly demonstrated. The results showed that compaction reduced porosity, while increased tortuosity.
3. The proposed empirical models adequately predicted the variations of porosity and tortuosity with the grain depth.

REFERENCES

ASABE Standard.1998. ASAE S352.2: Moisture measurement – unground grain and seed. St Joseph Mich.: ASABE.

ASABE Standard.1996. ASAE R2011. D272.3: Resistance to airflow of grains, seeds, other agricultural products and perforated metal sheet. St Joseph Mich.: ASABE.

Cheng, X., Q. Zhang, X. Xiaojie, and S. Cuixia. 2015. Compressibility and equivalent bulk modulus of shelled corn. Biosystems Engineering 140: 91-97.

Dullien, F.A.L. 1992. Porous Media: Fluid Transport and Pore Structure. New York: Academic Press.

Garg, D. (2005). Modeling non-uniform airflow and its application for partial chilled aeration using PHAST-FEM. MS thesis. West Lafayette, Indiana: Purdue University.

Gbenga O., G. Griffiths, A. Atungulu, and S. Sadaka. 2016. CFD modeling of air flow distribution in rice bin storage system with different grain mass configurations. Biosystems Engineering 151:286-297.

Haque, E. 2011. Void fraction as a function of depth pressure drops of packed beds of porous formed by granular materials. Transaction of the ASAE 54(6): 2239-2243.

Hihinashvili R. and R. Blumenfeld. 2010. Structural characterization of porous and granular materials. International Conference on Water Resources. Barcelona: CIMNE.

Khatchatourian, O.A and D L. Savicki. 2004. Mathematical modelling of airflow in an aerated soya bean store under non-uniform conditions. Biosystems Engineering, 88(2), 201–211.

Lawrence, J., & Maier, D. E. (2011). Three-dimensional airflow distribution in a maize silo with peaked, levelled and cored grain mass configurations. Biosystems Engineering 110(3):321-329.

Lukaszuk, J., M. Molenda, J.Horabik,B.Szot, and M.D.Montross. 2008. Airflow resistance of wheat bedding as influenced by the filling method. J. Agric. Eng. Res. 54(2):50-57.

Neethirajan, S., C. Karunakaran., D.S.Jayas, and N.D.G. White. 2006. X- ray computed tomography image analysis to explain the airflow resistance differences in grain bulks. Biosystems Engineering 94: 545 - 555.

Nwaizu, C. and Q. Zhang. 2015. Characterizing tortuous airflow paths in a grain bulk by using smoke visualization. Canadian Biosystems Engineering 57 (3): 13-22.

Peng, S., H. Qinhong, D. Stefan, and M. Zhang. 2012. Using X-ray computed tomography in pore structure characterization for a Berea sandstone: Resolution effect. Journal of Hydrology 254-261.

Richard G., J.F. Cousin, A. Bruand and J. Guerif. 2001. Effect of compaction on the porosity of a silty soil: Influence on unsaturated hydraulic properties. European Journal Of soil Science 52: 49-58.

Robertson, A.G. and D.J. Campbell. 1997. Simple, low-cost image analysis of soil pore structure. J.agric. Eng. Res. 68:291-296.

Shedd, C. K. 1951. Some new data on resistance of grains to airflow. J. Agric. Eng. 32: 493-

495.

Thompson, S.A. and I.J. Ross. 1983. Compressibility and frictional coefficients of wheat. Transaction of ASAE 26(4): 1171-1176.

Vogel, H.J. and A. Kretzschmar. 1996. Topological characterization of pore space in soil- sample preparation and digital image processing. Geoderma 73: 23-38.

Yue, R. and Q. Zhang. 2017. A pore-scale model for predicting resistance to airflow in bulk grain. Biosystems Engineering 155:142-151.

Yun, J., Y. Yue, and B. Yu. 2010. A geometrical model for tortuosity of tortuous streamline in porous media with cylindrical. Chin. Phys. Lett. 27(10): 1047041-1047044.